MOLECULAR IMAGING AND BIOLOGY

Mol Imaging Biol (2019) 21:907–916
DOI: 10.1007/s11307-018-01310-5

Published Online: 7 January 2019

RESEARCH ARTICLE

PET Imaging of HER2-Positive Tumors with Cu-64-Labeled Affibody Molecules

Shibo Qi,[1,2] Susan Hoppmann,[2] Yingding Xu,[2] Zhen Cheng[2]

[1]*School of Environmental and Chemical Engineering, Tianjin Polytechnic University, Tianjin, 300387, China*
[2]*Molecular Imaging Program at Stanford (MIPS), Department of Radiology, and Bio-X Program, Canary Center at Stanford for Cancer Early Detection, Stanford University, Stanford, CA, 94305-5344, USA*

Abstract

Purpose: Previous studies has demonstrated the utility of human epidermal growth factor receptor type 2 (HER2) as an attractive target for cancer molecular imaging and therapy. An affibody protein with strong binding affinity for HER2, $Z_{HER2:342}$, has been reported. Various methods of chelator conjugation for radiolabeling HER2 affibody molecules have been described in the literature including N-terminal conjugation, C-terminal conjugation, and other methods. Cu-64 has recently been extensively evaluated due to its half-life, decay properties, and availability. Our goal was to optimize the radiolabeling method of this affibody molecule with Cu-64, and translate a positron emission tomography (PET) probe with the best *in vivo* performance to clinical PET imaging of HER2-positive cancers.

Procedures: In our study, three anti-HER2 affibody proteins-based PET probes were prepared, and their *in vivo* performance was evaluated in mice bearing HER2-positive subcutaneous SKOV3 tumors. The affibody analogues, Ac-Cys-$Z_{HER2:342}$, Ac-$Z_{HER2:342}$(Cys^{39}), and Ac-$Z_{HER2:342}$-Cys, were synthesized using the solid phase peptide synthesis method. The purified small proteins were site-specifically conjugated with the maleimide-functionalized chelator, 1,4,7,10-tetraazacyclododecane-1,4,7-tris- aceticacid-10-maleimidethylacetamide (maleimido-mono-amide-DOTA). The resulting DOTA-affibody conjugates were then radiolabeled with Cu-64. Cell uptake assay of the resulting PET probes, [^{64}Cu]DOTA-Cys-$Z_{HER2:342}$, [^{64}Cu]DOTA-$Z_{HER2:342}$(Cys^{39}), and [^{64}Cu]DOTA-$Z_{HER2:342}$-Cys, was performed in HER2-positive human ovarian SKOV3 carcinoma cells at 4 and 37 °C. The binding affinities of the radiolabeled peptides were tested by cell saturation assay using SKOV3 cells. PET imaging, biodistribution, and metabolic stability studies were performed in mice bearing SKOV3 tumors.

Results: Cell uptake assays showed high and specific uptake by incubation of Cu-64-labeled affibodies with SKOV3 cells. The affinities (K_D) of the PET radio probes as tested by cell saturation analysis were in the low nanomolar range with the ranking of [^{64}Cu]DOTA-Cys-$Z_{HER2:342}$ (25.2 ± 9.2 nM) ≈ [^{64}Cu]DOTA-$Z_{HER2:342}$-Cys (32.6 ± 14.7 nM) > [^{64}Cu]DOTA-$Z_{HER2:342}$(Cys^{39}) (77.6 ± 22.2 nM). *In vitro* stability and *in vivo* metabolite analysis study revealed that all three probes were stable enough for *in vivo* imaging applications, while [^{64}Cu]DOTA-Cys-$Z_{HER2:342}$ showed the highest stability. *In vivo* small-animal PET further demonstrated fast tumor targeting, good tumor accumulation, and good tumor to normal tissue contrast of all three probes. For [^{64}Cu]DOTA-Cys-$Z_{HER2:342}$, [^{64}Cu]DOTA-$Z_{HER2:342}$(Cys^{39}), and

Electronic supplementary material The online version of this article (https://doi.org/10.1007/s11307-018-01310-5) contains supplementary material, which is available to authorized users.

Correspondence to: Zhen Cheng; *e-mail:* zcheng@stanford.edu

[^{64}Cu]DOTA-$Z_{HER2:342}$-Cys, tumor uptake at 24 h are 4.0 ± 1.0 % ID/g, 4.0 ± 0.8 %ID/g, and 4.3 ± 0.7 %ID/g, respectively (mean ± SD, n = 4). Co-injection of the probes with non-labeled anti-HER2 affibody proteins confirmed *in vivo* specificities of the compounds by tumor uptake reduction.

Conclusions: The three Cu-64-labeled $Z_{HER2:342}$ analogues all display excellent HER2 targeting ability and tumor PET imaging quality. Although varied in the position of the radiometal labeling of these three Cu-64-labeled $Z_{HER2:342}$ analogues, there is no significant difference in tumor and normal tissue uptakes among the three probes. [^{64}Cu]DOTA-Cys-$Z_{HER2:342}$ stands out as the most superior PET probe because of its highest affinities and *in vivo* stability.

Key words: PET, Affibody, HER2, Cu-64, Tumor

Introduction

Over the past decade, affibody protein scaffolds have been found to be a great platform for developing tumor targeting agents [1, 2]. Initially derived from the Z domain of staphylococcal protein A, affibody molecules are a class of binding proteins with high affinity. Affibody molecules are based on three-helix bundle scaffold structure and consist of 58-amino acid residues [1, 3]. Randomization of the 13 amino acid residues in helices 1 and 2 of an affibody molecule can be used to develop affibody proteins that possess high affinity for a variety of targets [4, 5]. Because of their small sizes and high affinities, affibody proteins have been characterized by rapid targeting, high uptake, and quick clearance, all of which facilitate high-contrast imaging. Importantly, the high affinity and specificity can be preserved through the synthetic process of conventional solid phase peptide synthesis. Recently, a variety of affibody proteins have been developed, targeting human epidermal growth factor receptor 2 (HER2), epidermal growth factor receptor 1 (EGFR), and others [1, 6]. For imaging applications, one can also label affibody molecules with a variety of organic dyes, nanoparticles, and radionuclides [6–8]. Overall, affibody molecules have been shown to have great potentials in theragnostics for cancer therapy.

Human epidermal growth factor receptor type 2 (HER2) is a well-established tumor target overexpressed in a wide range of cancers, particularly breast, ovarian, and lung cancers, among others [1, 9–11]. HER2 has seen many clinical applications over the past decade including therapy monitoring, prognosticating cancer patients, and acting as a molecular target for specific cancer therapies [1, 2, 12]. Numerous radionuclides including F-18 [7, 13–17], Tc-99m [18–20], In-111 [21, 22], Y-90 [23], Lu-177 [23, 24], I-125 [25, 26], Cu-64 [27], Ga-68 [28, 29], Re-188 [30], Sc-44 [31], and others have been used to label the anti-HER2 affibody (Z_{HER2}) molecules for tumor imaging or radionuclide therapy. In these studies, combinations of a variety of radionuclides, labeling chemistry, and affibody molecules have been explored in order to obtain radiolabeled Z_{HER2} molecules with optimal *in vivo* performance for clinical translation.

The binding segment of affibody proteins consists of 13 amino acid residues at the surface of the protein. They are located in the N-terminal helices 1 and 2 while the third helix contributes to the structural rigidity and stability of the molecule [6, 32] (Fig. 1). Various methods of chelator conjugation with Z_{HER2} molecules have been described in the literature including maleimide-sulfhydryl chemistry-based site-specific conjugation (both N-terminal and C-terminal cysteine residues have been targeted) as well as other radiolabeling methods through the conjugation with the lysine residues presented in the affibodies [21, 22, 25]. However, thus far, there has been no study to systematically study the impact of labeling affibodies with Cu-64 at different positions to their *in vivo* performance. In this study, by using a high-affinity anti-HER2 affibody binder $Z_{HER2:342}$ with a K_D of 22 pM as the template protein [25], Ac-Cys-$Z_{HER2:342}$ (where cysteine is placed in the N-terminal), Ac-$Z_{HER2:342}$(Cys39) (where the glutamine residue at position 39 is substituted by cysteine), and Ac-$Z_{HER2:342}$-Cys (where cysteine is placed in the C-terminal) (Fig. 1) were designed and radiolabeled with Cu-64 to systematically evaluate the effect of labeling sites to *in vivo* behaviors.

The three $Z_{HER2:342}$ molecules were synthesized by the traditional solid phase peptide synthesis method and then site-specifically modified at cysteine residues with the maleimide-functionalized chelator, 1,4,7,10-tetraazacyclododecane-1,4,7-tris- aceticacid-10-maleimidethylacetamide (maleimido-mono-amide-DOTA). The resulting DOTA-affibody bioconjugates, DOTA-Cys-$Z_{HER2:342}$, DOTA-$Z_{HER2:342}$(Cys^{39}), and DOTA-$Z_{HER2:342}$-Cys, were radiolabeled with the positron emitter Cu-64 ($t_{1/2}$ = 12.7 h, E_β^+max = 656 *ke*V, 17.8 %). Finally, the resulting positron emission tomography (PET) probes, [^{64}Cu]DOTA-Cys-$Z_{HER2:342}$, [^{64}Cu]DOTA-$Z_{HER2:342}$(Cys^{39}), and [^{64}Cu]DOTA-$Z_{HER2:342}$-Cys (Fig. 1), were evaluated in mice bearing subcutaneous HER2-positive SKOV3 tumors.

Materials and Methods

General

All standard chemicals were purchased from Sigma-Aldrich Chemical Co. (St. Louis, MO). Cu-64 was obtained from the Department of Medical Physics, University of Wisconsin at Madison (Madison, WI). Analytical reversed-phase high-

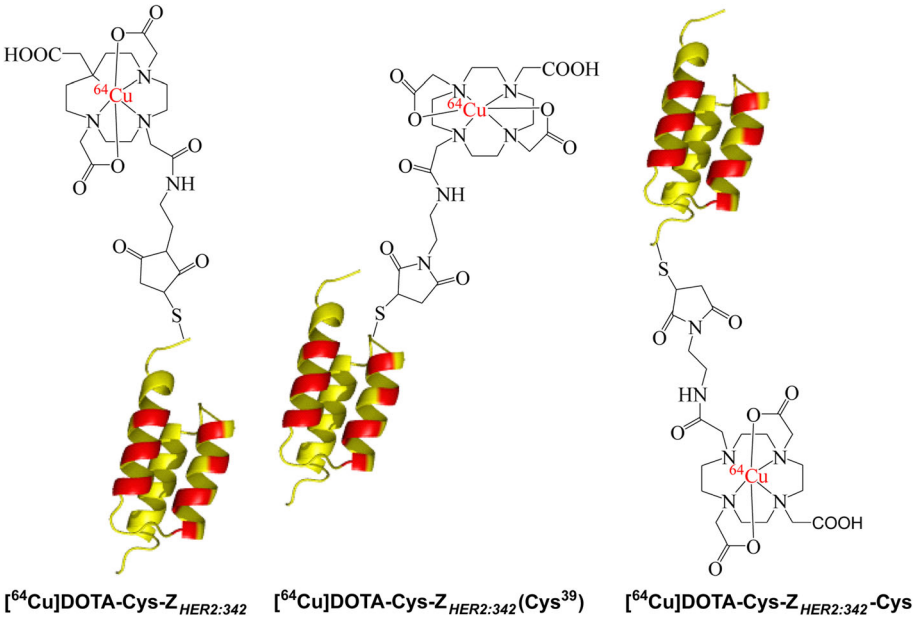

Fig. 1. Schematic structures of anti-HER2 affibody proteins-based radio probes.

performance liquid chromatography (RP-HPLC) column (Dionex, Acclaim-120 C18, 4.6 mm 250 mm) with a guard column was used for analysis of Cu-64-labeled and Cu-64-unlabeled affibodies. Stanford Protein and Nucleic Acid Biotechnology Facility (Stanford, CA) performed matrix-assisted laser desorption/ionization time-of-flight mass spectrometry (MALDI-TOF-MS) using a Voyager-DE RP Biospectrometer (Perseptive; Framingham, MA). We obtained human ovarian cancer SKOV3 cell line from the American Type Tissue Culture Collection (Manassas, VA). Female athymic nude mice (nu/nu) were from Charles River Laboratories (Boston, MA).

Synthesis of $Z_{HER2:342}$ Affibodies and Conjugation with DOTA

The affibody molecules [Ac-Cys-$Z_{HER2:342}$: Ac-CVDNKFNKEMRNAYWEIALLP NLNNQQKRAFIR SLYDDPSQSANLLAEAKKLNDAQAPK-NH_2); Ac-$Z_{HER2:342}$(Cys^{39}): Ac-VDNKFNKEMRNAYWEIA LLPNLNNQQKRAFIRSLYDDPCQSANLLAEAKKLND AQAPK-NH_2; and Ac-$Z_{HER2:342}$-Cys: Ac-VDNKFNKE MRNAYWEIALLPNLNNQQK RAFIRSLYDDPSQSAN LLAEAKKLNDAQAPKC-NH_2] were prepared on a solid phase peptide synthesizer (CS Bio, CS 336X, Palo Alto, CA) using the chemistry as previously reported [33]. The purified affibody molecules were characterized by MALDI-TOF-MS.

The affibody molecule [Cys-$Z_{HER2:34}$, $Z_{HER2:342}$(Cys^{39}), or $Z_{HER2:342}$-Cys] was dissolved in phosphate buffer (0.01 M, pH 7.4) freshly prepared at a concentration of 1 mg/ml. Then, the affibody was mixed with the bifunctional chelator maleimido-mono-amide-DOTA dissolved in DMSO (10 mM) at 1:15 equivalents. The reaction mixtures were vortexed for 2 h, and then they were injected into the Dionex HPLC with a C4 column for purification. The resulted products were characterized by MALDI-TOF-MS, and the purities of the bioconjugates were evaluated by HPLC.

Cu-64 Radiolabeling

The affibody conjugate [DOTA-Cys-$Z_{HER2:342}$, DOTA-$Z_{HER2:342}$(Cys^{39}), or DOTA-$Z_{HER2:342}$-Cys] was then radiolabeled with Cu-64. Specifically, $^{64}CuCl_2$ (83.3 MBq, 2.5 mCi, 1 μg of the affibody conjugate per 2.96 MBq Cu-64) in 0.1 N sodium acetate (NaOAc, pH 6.0) buffer was added to the affibody, followed by a 1-h incubation at 40 °C. At the end of reaction, ethylenediaminetetraacetic acid (EDTA, 2 μl, 10 mM) was added, and the radiolabeled product was subsequently purified by a PD-10 column (GE Healthcare) using phosphate-buffered saline (PBS, pH 7.4) as eluant. The final labeled affibody proteins were passed through a 0.22-μm Millipore filter into a sterile vial for further experiments. Radioanalytical HPLC was used as quality control to analyze the purity of the Cu-64-labeled affibody molecules.

In Vitro Cell Assays

In vitro cell uptake assays of the Cu-64-labeled affibody molecule ([^{64}Cu]DOTA-Cys-$Z_{HER2:342}$ (a), [^{64}Cu]DOTA-$Z_{HER2:342}$(Cys^{39}) (b), or [^{64}Cu]DOTA-$Z_{HER2:342}$-Cys (c) were carried as previously described [7]. In short, SKOV3 cells (2×10^5 per well) were seeded in 12-well tissue culture plates. These cells were allowed to grow overnight. After washing twice with the serum-free McCoy 5 medium, cells

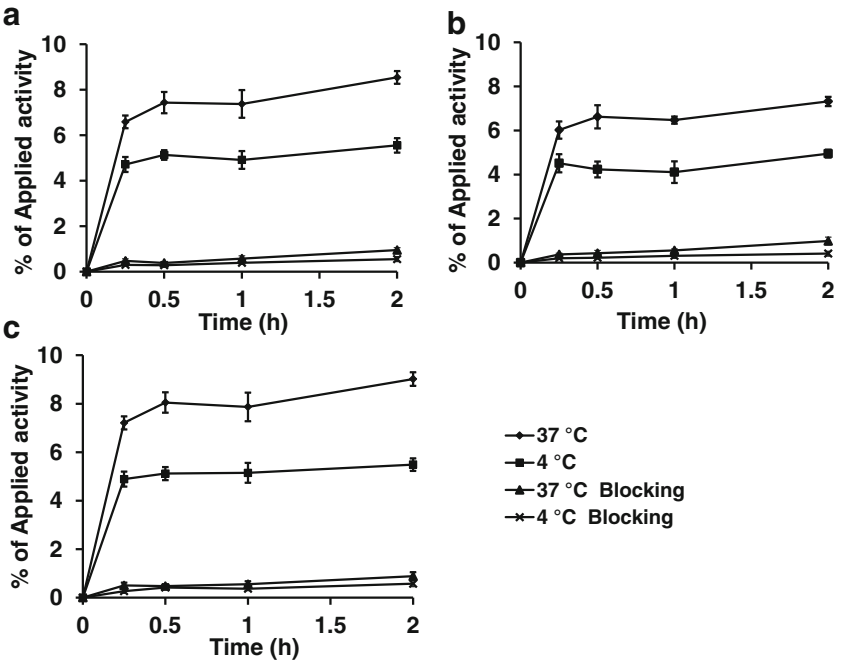

Fig. 2. Cell uptake of **a** [^{64}Cu]DOTA-Cys-$Z_{HER2:342}$, **b** [^{64}Cu]DOTA-$Z_{HER2:342}$(Cys^{39}), and **c** [^{64}Cu]DOTA-$Z_{HER2:342}$-Cys at 37 and 4 °C in SKOV3 cells over times at 4 and 37 °C in the presence or absence of nonradioactive affibody proteins.

were incubated with the Cu-64-labeled affibody probes (74 kBq per well, final concentration 6 nM) in 400 μl of medium at 4 and 37 °C. Co-incubation of the SKOV3 cells with the large excess of cold affibody molecule Ac-Cys-$Z_{HER2:342}$, Ac-$Z_{HER2:342}$(Cys^{39}), or Ac-$Z_{HER2:342}$-Cys (final concentration 600 nM) was applied to determine the nonspecific binding of the probes. At different incubation times (15, 30, 60, and 120 min), SKOV3 cells were washed three times with cold PBS and lysed with NaOH (200 μl, of 0.2 M). The collected lysed samples were counted using a PerkinElmer 1470 automatic γ-counter (Waltham). The cell uptake of the radiolabeled affibody was expressed as the percentage of added radioactivity.

The receptor saturation assay of the Cu-64-labeled affibody molecule ([^{64}Cu]DOTA-Cys-$Z_{HER2:342}$, [^{64}Cu]DOTA-$Z_{HER2:342}$(Cys^{39}), or [^{64}Cu]DOTA-$Z_{HER2:342}$-Cys) was conducted with the SKOV3 cells, and 2×10^5 cells were plated per well on 12-well plates 1 day before the experiment. Cells were washed with PBS three times. Serum-free McCoy 5 (1 ml) was added to each well, and 8.9–532.8 kBq (0.24–14.4 μCi, 2–120 nM final concentration) of the Cu-64-labeled affibody ([^{64}Cu]DOTA-Cys-$Z_{HER2:342}$, [^{64}Cu]DOTA-$Z_{HER2:342}$(Cys^{39}), or [^{64}Cu]DOTA-$Z_{HER2:342}$-Cys) with or without 1000 times excess of the nonradioactive affibody molecule Ac-Cys-$Z_{HER2:342}$, Ac-$Z_{HER2:342}$(Cys^{39}), or Ac-$Z_{HER2:342}$-Cys. The plates were incubated on ice for 2 h. Then, cells were washed with cold PBS three times and lysed with the addition of 200 μl of 0.2 M NaOH. The radioactivity of the cells was measured in the γ-counter. The data was analyzed using GraphPad Prism (GraphPad Software, Inc., San Diego, CA, USA), and the K_D value of the Cu-64-labeled affibody molecule was calculated from a one-site fit binding curve.

Serum Stability

The Cu-64-labeled affibody molecule ([^{64}Cu]DOTA-Cys-$Z_{HER2:342}$, [^{64}Cu]DOTA-$Z_{HER2:342}$(Cys^{39}), or [^{64}Cu]DOTA-$Z_{HER2:342}$-Cys) (6.7 MBq, 180 μCi) was mixed with mouse serum (1 ml). The serum solution (74–118 kBq, 20–40 μCi) was precipitated using ethanol (300 μl) after incubating it at 37 °C for different times (2, 4, and 24 h). DMF (300 μl) was added to the supernatant after centrifugation to precipitate the serum protein residue. Acidification of the supernatant was then performed with 300 μl of buffer A (0.1 % TFA in water) after centrifugation and filtered through a Spin-X centrifuge tube filter (0.22 μm nylon, COSTAR). The filtrate was then injected into radio-HPLC under the same conditions used for analyzing original the Cu-64-labeled affibody molecules.

Small-Animal PET and Biodistribution Studies

Animal studies were performed based on the protocol approved by the Stanford University Administrative Panels on Laboratory Animal Care (APLAC).

Implantation of SKOV3 cells suspended in PBS (3×10^6) in the right shoulders of female athymic nu/nu mice was performed. We allowed tumors to grow to a size of 0.5–0.7 cm in diameter, which usually took about 3 to 4 weeks. Imaging and biodistribution studies were then performed on the animals. Small-animal PET ($n = 4$ per group) was carried out using a micro-PET R4 scanner (Siemens Medical Solutions USA, Inc.). SKOV3 tumors mice were injected *via* the tail vein with 77–96 μCi (2.85–3.55 MBq, 0.96–1.2 μg) of the Cu-64-labeled affibody molecule ([^{64}Cu]DOTA-Cys-$Z_{HER2:342}$, [^{64}Cu]DOTA-

$Z_{HER2:342}$(Cys^{39}), or [^{64}Cu]DOTA-$Z_{HER2:342}$-Cys) with or without 300 μg of the affibody protein Ac-Cys-$Z_{HER2:342}$, Ac-$Z_{HER2:342}$(Cys^{39}), or Ac-$Z_{HER2:342}$-Cys, respectively. At various time points postinjection (p.i.) (0.5, 1, 2, 4, and 24 h), the mice anesthetized with 2 % isoflurane were placed in the prone position near the center of the field of view (FOV) of the small-animal PET. The mice were scanned for 5 min and two-dimensional ordered subsets expectation maximum (OSEM) algorithm was used to reconstruct the images. Lastly, the previously reported method was used to perform quantification analysis of small-animal PET images [27].

For biodistribution studies, immediately after small-animal PET imaging study at 24 h, the tumor-bearing mice were euthanized. Tumor and normal tissues were excised and weighed, followed by measuring their radioactivity by the γ-counter. The radioactivity uptake in different organs and tumor was expressed as percentage of injected dose per gram of tissue (% ID/g).

In Vivo Metabolic Analysis

The *in vivo* metabolic fate of the Cu-64-labeled affibody molecule ([^{64}Cu]DOTA-Cys-$Z_{HER2:342}$, [^{64}Cu]DOTA-$Z_{HER2:342}$(Cys^{39}), or [^{64}Cu]DOTA-$Z_{HER2:342}$-Cys) was studied from urine and tumor samples of tumor-bearing mice using previously reported procedures [15]. Following injecting the PET probe into the mice bearing SKOV3 tumor *via* the tail vein, the mice were euthanized at 2 h p.i. Different organs such as the liver, kidney, and tumor were homogenized and treated with DMF and PBS sequentially (500 μl each). The extracted solution was then centrifuged using a Costar nylon filter tube; the final prepared samples were further injected into the radio-HPLC for analysis. HPLC fractions at 0.5-min intervals were collected for tumor, kidney and liver extracts and counted by the γ-counter.

Statistical Method

Statistical analysis was performed using the two-tailed Student's *t* test for unpaired data. A 95 % confidence level was chosen to determine the significance between groups, with $P < 0.05$ being designated as significantly different. Correlation was conducted on graphs-prism with the best-fit linear regression line, with $P < 0.05$ being designated as correlated.

Results

Chemistry and Radiochemistry

The affibody protein [Ac-Cys-$Z_{HER2:342}$, Ac-$Z_{HER2:342}$(Cys^{39}), or Ac-$Z_{HER2:342}$-Cys] was successfully synthesized using the peptide synthesizer, and purified by semipreparative HPLC. The peptides were generally obtained in 2 % yield with over 95 % purity (Fig. S1a; see Electronic Supplementary Material (ESM)). The purified peptides were characterized by MALDI-TOF-MS, and the measured molecular weights (MW) were consistent with the expected values (Table 1). Maleimido-mono-amide-DOTA was then conjugated with the affibody molecules and the products were purified by C4 analytical HPLC. MALDI-TOF-MS analysis verified the successful preparation of the final products, DOTA-Cys-$Z_{HER2:342}$, DOTA-$Z_{HER2:342}$(Cys^{39}), and DOTA-$Z_{HER2:342}$-Cys (Table 1). The purities for the final products were all over 95 % (Fig. S1b, see ESM).

The affibody-DOTA conjugates [DOTA-Cys-$Z_{HER2:342}$, DOTA-$Z_{HER2:342}$(Cys^{39}), or DOTA-$Z_{HER2:342}$-Cys] were labeled with Cu-64 at 40 °C for a 1-h incubation. The labeling yields with Cu-64 were generally over 50 %. Purification of the radiolabeling solution using a PD-10 column provided probes ([^{64}Cu]DOTA-Cys-$Z_{HER2:342}$, [^{64}Cu]DOTA-$Z_{HER2:342}$(Cys^{39}), or [^{64}Cu]DOTA-$Z_{HER2:342}$-Cys) with > 95 % radiochemical purity (Fig. S1c, see ESM).

In Vitro Assay

The uptake of the radiolabeled affibody molecule ([^{64}Cu]DOTA-Cys-$Z_{HER2:342}$, [^{64}Cu]DOTA-$Z_{HER2:342}$(Cys^{39}), or [^{64}Cu]DOTA-$Z_{HER2:342}$-Cys) in SKOV3 cells over an incubation period of 2 h at 37 and 4 °C is shown in Fig. 2. All three radiolabeled peptides quickly accumulated in SKOV3 cells and steadily increased over the 2-h incubation period. The uptake for [^{64}Cu]DOTA-Cys-$Z_{HER2:342}$, [^{64}Cu]DOTA-$Z_{HER2:342}$ (Cys^{39}), and [^{64}Cu]DOTA-$Z_{HER2:342}$-Cys are 6.6 ± 0.3 %, 6.0 ± 0.4 %, and 7.2 ± 0.4 % at 0.25 h at 37 °C, and 8.5 ± 0.3 %, 7.3 ± 0.2 %, and 9.0 ± 0.3 % at 2 h at 37 °C, respectively (mean ± SD, $n = 3$). Importantly, co-incubation with large excess of the cold affibody molecules significantly blocked the radiolabeled affibody molecule uptake ($P < 0.05$) and thereby demonstrating the receptor-binding specificity of all three PET probes.

The receptor-binding affinity study of the PET probes ([^{64}Cu]DOTA-Cys-$Z_{HER2:342}$, [^{64}Cu]DOTA-$Z_{HER2:342}$(Cys^{39}), or [^{64}Cu]DOTA-$Z_{HER2:342}$-Cys) for HER2 was performed using SKOV3 cells. The K_D values of them are 25.2 ± 9.2, 77.6 ± 22.2, and 32.6 ± 14.7 nM, respectively (Table 1, Fig. S2, see ESM).

The serum stability study further showed that all three PET probes ([^{64}Cu]DOTA-Cys-$Z_{HER2:342}$, [^{64}Cu]DOTA-$Z_{HER2:342}$(Cys^{39}), or [^{64}Cu]DOTA-$Z_{HER2:342}$-Cys) had excellent resistance to proteolysis and transchelation with > 90 % of the probes intact after 2 h incubation in the serum, and there were approximately 50–65 % intact radio probes after 24 h of incubation (Fig. S3, see ESM).

In Vivo Metabolic Analysis

The *in vivo* metabolic fate of the PET probes ([^{64}Cu]DOTA-Cys-$Z_{HER2:342}$, [^{64}Cu]DOTA-$Z_{HER2:342}$(Cys^{39}), or [^{64}Cu]DOTA-$Z_{HER2:342}$-Cys) in the SKOV3 tumor mice was determined and the results are shown in Fig. 3. At 2 h p.i., the percentages of intact

probes in the tumor for [^{64}Cu]DOTA-Cys-$Z_{HER2:342}$, [^{64}Cu]DOTA-$Z_{HER2:342}$(Cys^{39}), and [^{64}Cu]DOTA-$Z_{HER2:342}$-Cys were 84.8, 69.0, and 67.7 %, respectively. In the kidney and liver, all three PET probes were almost completely metabolized at 2 h p.i.

Small-Animal PET and Biodistribution Studies

PET imaging studies were conducted after tail vein injection of the PET probes ([^{64}Cu]DOTA-Cys-$Z_{HER2:342}$, [^{64}Cu]DOTA-$Z_{HER2:342}$(Cys^{39}), or [^{64}Cu]DOTA-$Z_{HER2:342}$-Cys) with and without co-injection of 300 μg (blocking) of cold affibody molecules [Ac-Cys-$Z_{HER2:342}$, Ac-$Z_{HER2:342}$(Cys^{39}), or Ac-$Z_{HER2:342}$-Cys], respectively. Decay-corrected coronal small-animal PET images are shown in Fig. 4. For all three probes, the SKOV3 tumor was clearly visualized and differentiated from background tissue from 0.5 to 24 h p.i. (Fig. 4a–c). By comparison, the tumor was barely visible on PET images at 1 h p.i. for the blocking groups (Fig. 4d). Also, high activity accumulation in the kidneys for the three probes was observed in all images (Fig. 4a, b). Quantification analysis revealed that for [^{64}Cu]DOTA-Cys-$Z_{HER2:342}$, [^{64}Cu]DOTA-$Z_{HER2:342}$(Cys^{39}), and [^{64}Cu]DOTA-$Z_{HER2:342}$-Cys, tumor uptakes were 4.0 ± 1.0 %ID/g, 4.0 ± 0.8 %ID/g, and 4.3 ± 0.7 %ID/g at 24 h p.i., respectively (mean ± SD, n = 4, Fig. 4e). Moreover, PET quantification analysis showed slow washout of the probes from tumor: even after 24 h, high tumor accumulation was observable in the PET images (Fig. 4).

Table 1.. The expected and measured molecular weight (M.W.) of the affibody molecules and the DOTA-affibody conjugates for $[M + H]^+$ by MALDI-TOF-MS, and K_D values of the three PET probes

Peptides or probes	Expected M.W.	Measured M.W.	K_D (nM)
Ac-Cys-$Z_{HER2:342}$	6849.8	6850.9	
Ac-$Z_{HER2:342}$(Cys^{39})	6762.7	6763.7	
Ac-$Z_{HER2:342}$-Cys	6849.8	6850.3	
DOTA-Cys-$Z_{HER2:342}$	7376.3	7374.8	
DOTA-$Z_{HER2:342}$(Cys^{39})	7289.5	7289.7	
DOTA-$Z_{HER2:342}$-Cys	7376.3	7375.9	
[^{64}Cu]DOTA-Cys-$Z_{HER2:342}$			25.2 ± 9.2
[^{64}Cu]DOTA-$Z_{HER2:342}$(Cys^{39})			77.6 ± 22.2
[^{64}Cu]DOTA-$Z_{HER2:342}$-Cys			32.6 ± 14.7

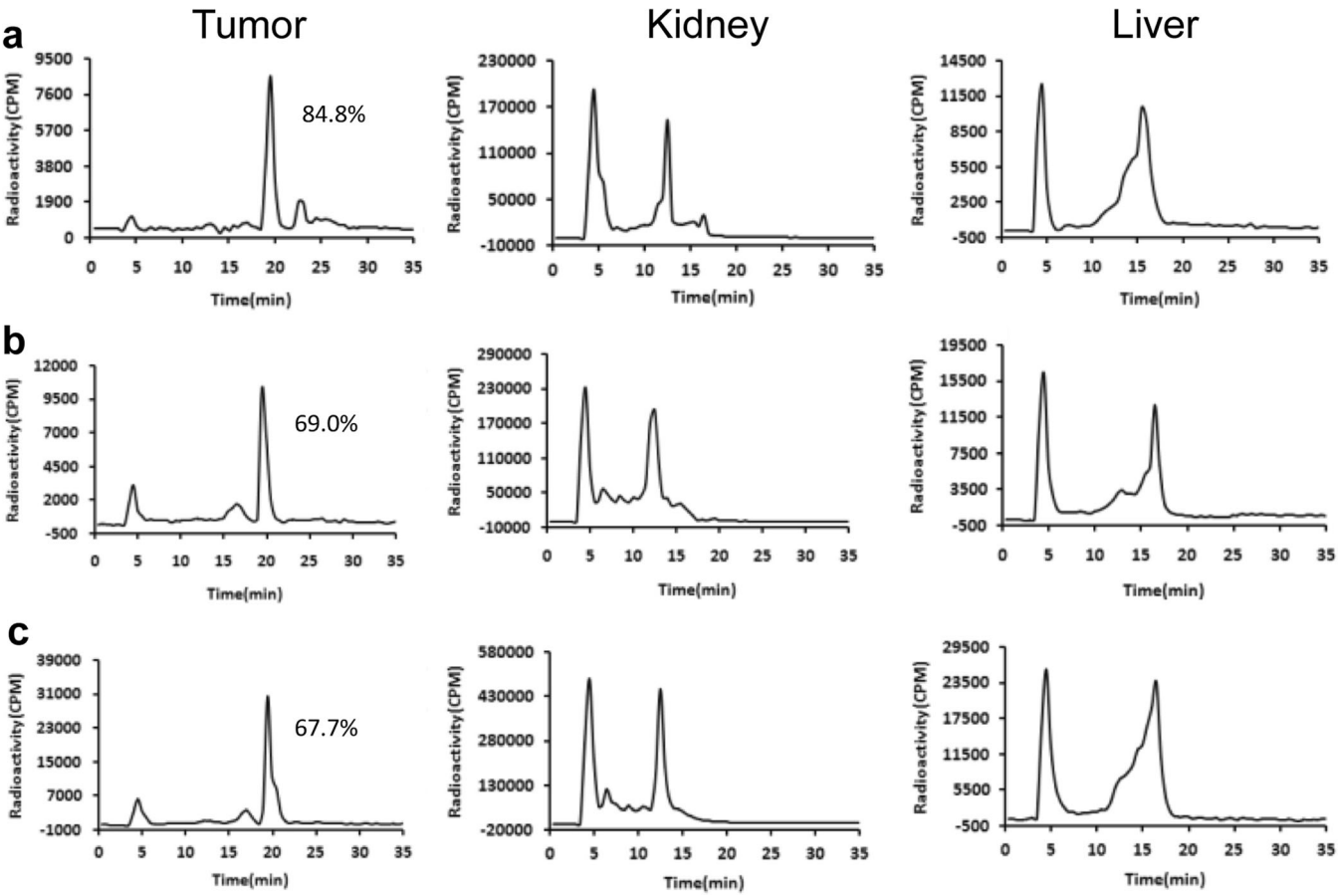

Fig. 3. *In vivo* metabolic stability study of **a** [^{64}Cu]DOTA-Cys-$Z_{HER2:342}$, **b** [^{64}Cu]DOTA-$Z_{HER2:342}$(Cys^{39}), and **c** [^{64}Cu]DOTA-$Z_{HER2:342}$-Cys at 2 h postinjection. Samples were taken from the tumor (left column), kidney (center column), and liver (right column). Percentages of intact probes are calculated from the area under the curve and are shown in the corresponding panels. In the kidney and liver, the percentage is not shown, given the complete degradation of the probes.

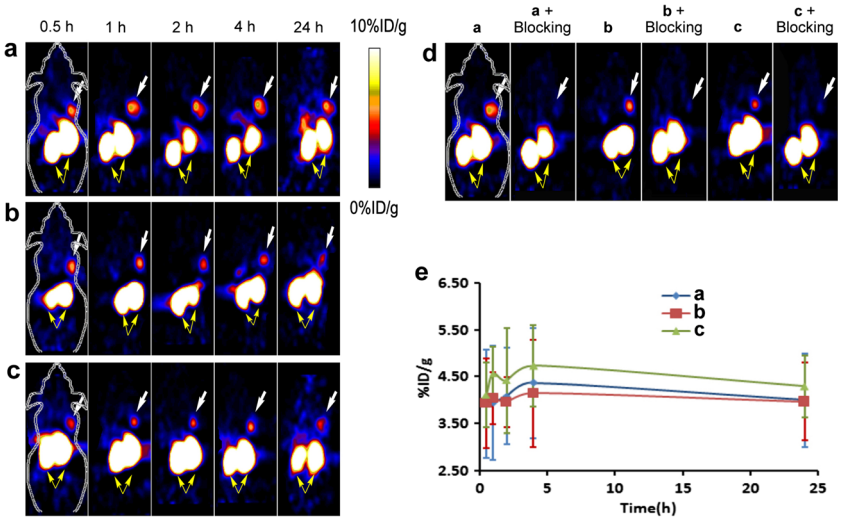

Fig. 4. Representative decay-corrected coronal PET images at 0.5, 1, 2, 4, and 24 h after tail vein injection of **a** [^{64}Cu]DOTA-Cys-$Z_{HER2:342}$, **b** [^{64}Cu]DOTA-$Z_{HER2:342}$(Cys^{39}), or **c** [^{64}Cu]DOTA-$Z_{HER2:342}$-Cys. White arrows indicate the location of the tumors, and yellow arrows indicate the location of the kidneys. **d** Representative decay-corrected coronal PET images at 1 h after tail vein injection of the three PET probes (**a**, **b**, or **c**) without or with (blocking) affibody proteins, Ac-Cys-$Z_{HER2:342}$, Ac-$Z_{HER2:342}$(Cys^{39}), or Ac-$Z_{HER2:342}$-Cys. **e** Uptake levels of tumor derived from multiple time points small-animal PET images after tail vein injection of the probes (**a**, **b**, or **c**). Data are shown as mean ± SD of four measurements.

data of the three probes and blocking groups are shown in Fig. 5. For the three PET probes, high levels of radioactivity accumulation in the HER2-overexpressing SKOV3 tumors were observed (for [^{64}Cu]DOTA-Cys-$Z_{HER2:342}$, [^{64}Cu]DOTA-$Z_{HER2:342}$(Cys^{39}), and [^{64}Cu]DOTA-$Z_{HER2:342}$-Cys), tumor uptakes were 7.6 ± 3.0 %ID/g, 7.7 ± 0.8 %ID/g, and 6.6 ± 1.2 %ID/g at 24 h p.i., respectively, with data expressed as mean ± SD, n = 4). The tumor uptakes of the probes were significantly lower in the blocking groups (for [^{64}Cu]DOTA-Cys-$Z_{HER2:342}$, [^{64}Cu]DOTA-$Z_{HER2:342}$(Cys^{39}), and [^{64}Cu]DOTA-$Z_{HER2:342}$-Cys), tumor uptakes were 2.4 ± 0.4 %ID/g, 1.7 ± 0.4 %ID/g, and 2.5 ± 0.5 %ID/g at 24 h p.i., respectively, with data expressed as mean ± SD, n = 4, compared with the non-blocking group $P < 0.05$). There was a large fraction of the three probes accumulated in the kidneys in all tumor-bearing mice. Kidney uptakes are very high and are not shown in Fig. 5 because the values are out of scale of uptakes from the rest of the organs. Briefly, in the kidneys, the uptakes of [^{64}Cu]DOTA-Cys-$Z_{HER2:342}$, [^{64}Cu]DOTA-$Z_{HER2:342}$(Cys^{39}), and [^{64}Cu]DOTA-$Z_{HER2:342}$-Cys were 97.9 ± 10.1 %ID/g, 116.1 ± 25.9 %ID/g, and 76.7 ± 6.6 %ID/g, respectively (mean ± SD %ID/g).

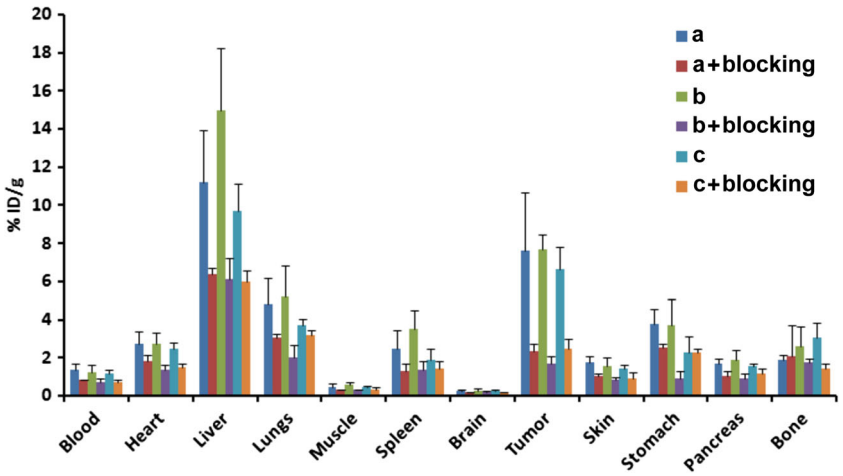

Fig. 5. Uptake levels of the blood, heart, liver, muscle, spleen, brain, tumor, skin, stomach, pancreas, and bone at 24 h after tail vein injection of [^{64}Cu]DOTA-Cys-$Z_{HER2:342}$ (**a**), [^{64}Cu]DOTA-$Z_{HER2:342}$(Cys^{39}) (**b**), or [^{64}Cu]DOTA-$Z_{HER2:342}$-Cys (**c**) without or with (blocking) affibody proteins, Cys-$Z_{HER2:342}$, $Z_{HER2:342}$(Cys^{39}), or $Z_{HER2:342}$-Cys. Data are shown as mean ± SD of four measurements.

Discussion

Due to its high sensitivity, good spatial resolution, and accurate quantification, PET, a non-invasive molecular imaging technology, has been widely utilized to address many important clinical questions in oncology [34]. Molecular probes for HER2 imaging have been applied in early detection of HER2-positive tumor, stratification of cancer patients, and prediction of the patients' sensitivity to anti-HER2 treatment [1, 2]. Over the past decade, affibody has been demonstrated to be a promising platform for developing a molecular imaging probe to target HER2 or epidermal growth factor receptor (EGFR) proteins [1, 12]. In this study, three $Z_{HER2:342}$ analogues, Ac-Cys-$Z_{HER2:342}$, Ac-$Z_{HER2:342}$(Cys^{39}), and Ac-$Z_{HER2:342}$-Cys, were successfully synthesized by the solid phase peptide synthesis method.

By taking advantage of well-established maleimide-sulfhydryl chemistry [35], the maleimide-functionalized chelator (Mal-DOTA) was site-specifically conjugated to the three cysteine-containing $Z_{HER2:342}$ molecules for radiometal labeling purposes. The chelator Mal-DOTA has been demonstrated in multiple studies to have the capability of site-specific conjugation with the thiol group in the cysteine residues of the affibody. While $Z_{HER2:342}$ and H_6-$Z_{HER2:342}$ were used in the previously published literature [35], three homogeneous $Z_{HER2:342}$ analogues were used in this study with varying positions of the maleimide-functionalized chelator including the C-terminus, the N-terminus as well as position 39 at the junction of helices 1 and 2, thanks to the site-specificity of Mal-DOTA. Of note, position 39 is located at the junction between helices 2 and 3. It is generally believed that the further away the labeling site is from the surface-exposed binding sequences, namely, helices 1 and 2, the less the binding affinity will be affected by radiolabeling. Therefore, Ac-$Z_{HER2:342}$(Cys^{39}) was designed to add to testing this running hypothesis.

As a nontraditional positron-emitting radionuclide, Cu-64 has recently been extensively evaluated due to its half-life (12.7 h), decay properties (β^+, 0.653 MeV, 17.8 %; β^-, 0.579 MeV, 38.4 %; the remainder is electron capture), and effective production by both reactor-based and accelerator-based methods [36, 37]. Furthermore, different chelators for copper radionuclide in PET have been effectively synthesized, which can potentially be linked to peptides, proteins, antibodies, and other biologically relevant molecules [37, 38]. Therefore, in this study, three chelator-cysteine-affibody conjugates [DOTA-Cys-$Z_{HER2:342}$, DOTA-$Z_{HER2:342}$(Cys^{39}), or DOTA-$Z_{HER2:342}$-Cys] were radiolabeled with Cu-64 for PET imaging of HER2-positive tumors.

The *in vitro* cell uptake experiment shows that all three probes have rapid and similar accumulation in the SKOV3 cells. The uptakes reach a plateau in 15 min at 37 °C. Furthermore, the accumulation is HER2 specific since blocking with the corresponding $Z_{HER2:342}$ analogue can significantly reduce the cell uptakes of the probe (Fig. 2). Cell saturation analysis reveals that the three probes preserve high binding affinities to HER2 (all in low nanomolar range). Interestingly, the ranking of the binding affinity of the three probes is [^{64}Cu]DOTA-Cys-$Z_{HER2:342}$ (25.2 ± 9.2 nM) ≈ [^{64}Cu]DOTA-$Z_{HER2:342}$-Cys (32.6 ± 14.7 nM) > [^{64}Cu]DOTA-$Z_{HER2:342}$(Cys^{39}) (77.6 ± 22.2 nM) (Table 1, Fig. S2). Though conjugation of $Z_{HER2:342}$ with a relatively small metal chelator at different positions leads to probes with good binding affinities in general, modification at the N- or C-terminus of $Z_{HER2:342}$ seems to be a better option than that of position 39, which is at the junction between helices 2 and 3. Yet the running hypothesis that the further away the radiolabeling site is from the surface-exposed residues the better the binding affinity of radiolabeled affibody molecules seems problematic in this case as the analogue with presumably the most interfering radiolabeling at the N-terminus of helix 1, [^{64}Cu]DOTA-Cys-$Z_{HER2:342}$, did not show any inferiority to the radiolabeling at the C-terminus of helix 3, [^{64}Cu]DOTA-$Z_{HER2:342}$-Cys.

Stability of [^{64}Cu]DOTA-Cys-$Z_{HER2:342}$, [^{64}Cu]DOTA-$Z_{HER2:342}$(Cys^{39}), and [^{64}Cu]DOTA-$Z_{HER2:342}$-Cys is also tested at different time points. In mouse serum, all three probes exhibit excellent stability with > 90 % of probes intact at 2 h. But at later time points (4 and 24 h), [^{64}Cu]DOTA-Cys-$Z_{HER2:342}$ appears to be more stable than [^{64}Cu]DOTA-$Z_{HER2:342}$(Cys^{39}) and [^{64}Cu]DOTA-$Z_{HER2:342}$-Cys (64.3 % *vs.* 51.5 and 49.7 %, Fig. S3). Moreover, *in vivo* metabolic assay demonstrates that at 2 h the percentages of intact probes in tumor were 84.8 % for [^{64}Cu]DOTA-Cys-$Z_{HER2:342}$, 69.0 % for [^{64}Cu]DOTA-$Z_{HER2:342}$(Cys^{39}), and 67.7 % for [^{64}Cu]DOTA-$Z_{HER2:342}$-Cys, which is consistent with the results obtained from the *in vitro* mouse serum stability study (Fig. 3). The greater extent of probe degradation *in vivo* when compared with *in vitro* are also expected. What is also interesting is the fact that in the kidney and liver, all three PET probes are almost completely metabolized at 2 h p.i.. Overall, these data indicate that modification of $Z_{HER2:342}$ yields [^{64}Cu]DOTA-Cys-$Z_{HER2:342}$ with the highest *in vitro* and *in vivo* stability among the three probes tested. It is unclear why this particular probe appears to be superior than the other two probes but the subtle structural difference regarding positions of radiometal labeling could indeed play a role.

Though some differences were observed for the affinities and stabilities of these three probes, good affinity (in low nM range) and stability at 2 h (> 90 %) already warrant their use for *in vivo* imaging. It is important to point out that good tumor imaging contrast is already achieved at 0.5 h p.i. for all the probes and thus regardless of the differential stability at 4 and 24 h, all three probes have been proved to be stable enough for *in vivo* imaging (Fig. 4). Furthermore, the three $Z_{HER2:342}$ analogues exhibit favorable *in vivo* pharmacokinetics. Good tumor imaging contrast can be obtained at as early as 0.5 h p.i. of the probes, and the tumor uptakes of the three tracers essentially maintained at the same level at all time points p.i. (Fig. 4c). Thus, Cu-64-labeled $Z_{HER2:342}$ analogues display rapid tumor accumulation and blood

clearance. These are major advantages for the use of these relatively small synthetic proteins as imaging agents compared to large, slow clearance proteins such as the intact antibodies. Of note, tumor uptakes of the probes were greatly reduced in the blocking groups, which confirmed targeting specificity (Fig. 4b and Fig. 5). Interestingly, it was found that [^{64}Cu]DOTA-$Z_{HER2:342}$-Cys (3) showed much lower kidney uptakes than that of [^{64}Cu]DOTA-Cys-$Z_{HER2:342}$ and [^{64}Cu]DOTA-$Z_{HER2:342}$-Cys; this may be caused by the lowest *in vivo* stability of this probe as the degraded fragments with small size could be easily cleared from the body.

The biodistribution results also revealed the very high kidney uptake and retention for the Cu-64-labeled affibody molecules. Interestingly, the blocking agent did not significantly reduce the renal uptake for probes [^{64}Cu]DOTA-Cys-$Z_{HER2:342}$ and [^{64}Cu]DOTA-$Z_{HER2:342}$-Cys, but it did significantly decrease probe [^{64}Cu]DOTA-$Z_{HER2:342}$(Cys^{39})'s renal uptake for 41 %. Further studies are required to clarify the potential mechanism for this observation. The radiation dose to the kidney, a radiation-sensitive organ, will likely be a concern for the use of the particularly high-energy Cu-64 probe clinically. The high uptake in the kidney is a well-known issue for antibody fragments, small protein and peptide-based probes especially labeled with radiometal. To reduce the potential renal toxicity, co-injection of the radioactive probe with positive charged amino acids such as lysine could be explored. Moreover, as the radiometal was used in the above study, their residualizing properties lead to the high uptake by the proximal tubule. The use of radiohalogens such as F-18, radioiodine could significantly reduce kidney accumulation and make the resulted HER2 affibody-based probes more suitable for clinical uses [14]. Lastly, modification of the surface charge, lipophilicity, and binding affinity can all be achieved by modifying the amino acid sequence of affibodies, which could provide yet another avenue to counter potential kidney toxicity.

Given the good *in vitro* and *in vivo* results, the three Cu-64-labeled $Z_{HER2:342}$ analogues could be used as candidates for further HER2 imaging studies. Especially [^{64}Cu]DOTA-Cys-$Z_{HER2:342}$ is the most superior probe of the three, considering its highest stability and binding affinity. Our results have also demonstrated that the binding affinity of an affibody-based probe is not the only factor determining its tumor localization; other properties of the probe such as chelator position, amino acid sequence, size, lipophilicity, and charge are also likely to play important roles for the probe's *in vivo* biological behavior. Many more affibody analogs are being synthesized and evaluated in our laboratory in order to further our understanding of the role of each of these probe characteristics.

Conclusion

Cu-64-labeled $Z_{HER2:342}$ analogues ([^{64}Cu]DOTA-Cys-$Z_{HER2:342}$, [^{64}Cu]DOTA-$Z_{HER2:342}$ (Cys^{39}), and [^{64}Cu]DOTA-$Z_{HER2:342}$-Cys) were successfully prepared. All three probes demonstrate good *in vitro* binding affinity and stability, while [^{64}Cu]DOTA-Cys-$Z_{HER2:342}$ displays the highest affinity and *in vivo* stability. Importantly, all these PET probes display excellent HER2 targeting ability and tumor PET imaging quality. Our results also highlight that although the position of the radiometal labeling of these three Cu-64-labeled $Z_{HER2:342}$ analogues vary, there is no significant difference in the tumor and normal tissue uptakes among the three probes. [^{64}Cu]DOTA-Cys-$Z_{HER2:342}$ stands out as the most superior PET probe thanks to its highest affinities and *in vivo* stability.

Acknowledgments. This work was supported, in part, by the Department of Radiology, Stanford University (ZC), National Cancer Institute (NCI) 5R01 CA119053 (ZC), a fellowship from China Scholarship Council (to SQ),Tianjin Municipal Education Commission 20140512 (SQ).

Compliance with Ethical Standards. Animal studies were performed based on the protocol approved by the Stanford University Administrative Panels on Laboratory Animal Care (APLAC).

Conflict of Interest

The authors declare that they have no conflict of interest.

References

1. Corcoran EB, Hanson RN (2014) Imaging EGFR and HER2 by PET and SPECT: a review. Med Res Rev 34:596–643
2. Parakh S, Gan HK, Parslow AC, Burvenich IJG, Burgess AW, Scott AM (2017) Evolution of anti-HER2 therapies for cancer treatment. Cancer Treat Rev 59:1–21
3. Löblom J, Feldwisch J, Tolmachev V et al (2010) Affibody molecules: engineered proteins for therapeutic, diagnostic and biotechnological applications. FEBS Lett 584:2670–2680
4. Miao Z, Levi J, Cheng Z (2011) Protein scaffold-based molecular probes for cancer molecular imaging. Amino Acids 41:1037–1047
5. Justino CIL, Duarte AC, Rocha-Santos TAP (2015) Analytical applications of affibodies. Trac-trend Anal Chem 65:73–82
6. Nilsson FY, Tolmachev V (2007) Affibody molecules: new protein domains for molecular imaging and targeted tumor therapy. Curr Opin Drug Discov Devel 10:167–175
7. Cheng Z, De Jesus OP, Namavari M et al (2008) Small-animal PET imaging of human epidermal growth factor receptor type 2 expression with site-specific ^{18}F-labeled protein scaffold molecules. J Nucl Med 49:804–813
8. Lee SB, Hassan M, Fisher R, Chertov O, Chernomordik V, Kramer-Marek G, Gandjbakhche A, Capala J (2008) Affibody molecules for in vivo characterization of HER2-positive tumors by near-infrared imaging. Clin Cancer Res 14:3840–3849
9. Meric-Bernstam F, Hung MC (2006) Advances in targeting human epidermal growth factor receptor-2 signaling for cancer therapy. Clin Cancer Res 12:6326–6330
10. Robert NJ, Favret AM (2007) HER2-positive advanced breast cancer. Hematol Oncol Clin North Am 21:293–302
11. Ferretti G, Felici A, Papaldo P, Fabi A, Cognetti F (2007) HER2/neu role in breast cancer: from a prognostic foe to a predictive friend. Curr Opin Obstet Gynecol 19:56–62
12. Ståhl S, Grälund T, Karlström AE et al (2017) Affibody molecules in biotechnological and medical applications. Trends Biotechnol 35:691–712
13. Namavari M, Padilla De Jesus O, Cheng Z et al (2008) Direct site-specific radiolabeling of an Affibody protein with 4-[^{18}F]fluorobenzaldehyde via oxime chemistry. Mol Imaging Biol 10:177–181

14. Kramer-Marek G, Kiesewetter DO, Martiniova L, Jagoda E, Lee SB, Capala J (2008) [^{18}F]FBEM-$Z_{HER2:342}$-Affibody molecule-a new molecular tracer for in vivo monitoring of HER2 expression by positron emission tomography. Eur J Nucl Med Mol Imaging 35:1008–1018
15. Miao Z, Ren G, Jiang L, Liu H, Webster JM, Zhang R, Namavari M, Gambhir SS, Syud F, Cheng Z (2011) A novel ^{18}F-labeled two-helix scaffold protein for PET imaging of HER2-positive tumor. Eur J Nucl Med Mol Imaging 38:1977–1984
16. Rosik D, Thibblin A, Antoni G, Honarvar H, Strand J, Selvaraju RK, Altai M, Orlova A, Eriksson Karlström A, Tolmachev V (2014) Incorporation of a triglutamyl spacer improves the biodistribution of synthetic affibody molecules radiofluorinated at the N-terminus via oxime formation with ^{18}F-4-fluorobenzaldehyde. Bioconjug Chem 25:82–92
17. Xu Y, Bai Z, Huang Q, Pan Y, Pan D, Wang L, Yan J, Wang X, Yang R, Yang M (2017) PET of HER2 expression with a novel ^{18}FAl labeled affibody. J Cancer 8:1170–1178
18. Orlova A, Nilsson FY, Wikman M et al (2006) Comparative in vivo evaluation of technetium and iodine labels on an anti-HER2 affibody for single-photon imaging of HER2 expression in tumors. J Nucl Med 47:512–519
19. Hofström C, Altai M, Honarvar H, Strand J, Malmberg J, Hosseinimehr SJ, Orlova A, Gräslund T, Tolmachev V (2013) HAHAHA, HEHEHE, HIHIHI, or HKHKHK: influence of position and composition of histidine containing tags on biodistribution of [^{99m}Tc(CO)$_3$]$^+$-labeled affibody molecules. J Med Chem 56:4966–4974
20. Zhang J, Zhao X, Wang S, Wang N, Han J, Jia L, Ren X (2015) Monitoring therapeutic response of human ovarian cancer to trastuzumab by SPECT imaging with ^{99m}Tc-peptide-$Z_{HER2:342}$. Nucl Med Biol 42:541–546
21. Tolmachev V, Nilsson FY, Widström C et al (2006) ^{111}In-benzyl-DTPA-$Z_{HER2:342}$, an affibody-based conjugate for in vivo imaging of HER2 expression in malignant tumors. J Nucl Med 47:846–853
22. Perols A, Honarvar H, Strand J, Selvaraju R, Orlova A, Eriksson Karlström A, Tolmachev V (2012) Influence of DOTA chelator position on biodistribution and targeting properties of ^{111}In-labeled synthetic anti-HER2 affibody molecules. Bioconjug Chem 23:1661–1670
23. Fortin MA, Orlova A, Malmstrom PU, Tolmachev V (2007) Labelling chemistry and characterization of [^{90}Y/^{177}Lu]-DOTA-$Z_{HER2:342-3}$ affibody molecule, a candidate agent for locoregional treatment of urinary bladder carcinoma. Int J Mol Med 19:285–291
24. Altai M, Westerlund K, Velletta J, Mitran B, Honarvar H, Karlström AE (2017) Evaluation of affibody molecule-based PNA-mediated radionuclide pretargeting: development of an optimized conjugation protocol and ^{177}Lu labeling. Nucl Med Biol 54:1–9
25. Orlova A, Magnusson M, Eriksson TLJ, Nilsson M, Larsson B, Höidén-Guthenberg I, Widström C, Carlsson J, Tolmachev V, Ståhl S, Nilsson FY (2006) Tumor imaging using a picomolar affinity HER2 binding affibody molecule. Cancer Res 66:4339–4348
26. Honarvar H, Westerlund K, Altai M et al (2012) Feasibility of affibody molecule-based PNA-mediated radionuclide pretargeting of malignant tumors. Theranostics 6:93–103
27. Cheng Z, De Jesus OP, Kramer DJ et al (2012) ^{64}Cu-labeled affibody molecules for imaging of HER2 expressing tumors. Mol Imaging Biol 12:316–324
28. Strand J, Honarvar H, Perols A, Orlova A, Selvaraju RK, Karlström AE, Tolmachev V (2013) Influence of macrocyclic chelators on the targeting properties of ^{68}Ga-labeled synthetic affibody molecules: comparison with ^{111}In-labeled counterparts. PLoS One 8:e70028
29. Sandberg D, Tolmachev V, Velikyan I, Olofsson H, Wennborg A, Feldwisch J, Carlsson J, Lindman H, Sörensen J (2017) Intra-image referencing for simplified assessment of HER2-expression in breast cancer metastases using the affibody molecule ABY-025 with PET and SPECT. Eur J Nucl Med Mol Imaging 44:1337–1346
30. Altai M, Honarvar H, Wållberg H, Strand J, Varasteh Z, Rosestedt M, Orlova A, Dunås F, Sandström M, Löfblom J, Tolmachev V, Ståhl S (2014) Selection of an optimal cysteine-containing peptide-based chelator for labeling of affibody molecules with ^{188}Re. Eur J Med Chem 87:519–528
31. Honarvar H, Müller C, Cohrs S, Haller S, Westerlund K, Karlström AE, van der Meulen NP, Schibli R, Tolmachev V (2017) Evaluation of the first ^{44}Sc-labeled affibody molecule for imaging of HER2-expressing tumors. Nucl Med Biol 45:15–21
32. Webster JM, Zhang R, Gambhir SS, Cheng Z, Syud FA (2009) Engineered two-helix small proteins for molecular recognition. Chembiochem 10:1293–1296
33. Qi S, Miao Z, Liu H, Xu Y, Feng Y, Cheng Z (2012) Evaluation of four affibody-based near-infrared fluorescent probes for optical imaging of epidermal growth factor receptor positive tumors. Bioconjug Chem 23:1149–1156
34. Massoud TF, Gambhir SS (2013) Molecular imaging in living subjects: seeing fundamental biological processes in a new light. Genes Dev 17:545–580
35. Ahlgren S, Orlova A, Rosik D, Sandström M, Sjöberg A, Baastrup B, Widmark O, Fant G, Feldwisch J, Tolmachev V (2008) Evaluation of maleimide derivative of DOTA for site-specific labeling of recombinant affibody molecules. Bioconjug Chem 19:235–243
36. Blower PJ, Lewis JS, Zweit J (1996) Copper radionuclides and radiopharmaceuticals in nuclear medicine. Nucl Med Biol 23:957–980
37. Shokeen M, Anderson CJ (2009) Molecular imaging of cancer with copper-64 raidiopharmaceuticals and positron emission tomography (PET). Accounts Chem Res 42:832–841
38. Cai Z, Anderson CJ (2013) Chelators for copper radionuclides in positron emission tomography radiopharmaceuticals. J Label Compd Radiopharm 57:224–230